

Supporting Information

Construction of Single-atom Copper Sites with Low Coordination Number for the Efficient CO₂ Electroreduction to CH₄

Shaomin Wei, Xingxing Jiang, Congyi He, Siyu Wang, Qi Hu, Xiaoyan Chai, Xiangzhong Ren, Hengpan Yang and Chuanxin He**

College of Chemistry and Environmental Engineering, Shenzhen University, Shenzhen, Guangdong, 518060, China

E-mail: hpyang@szu.edu.cn (H. Yang); hecx@szu.edu.cn (C. He)

Contents:

Supplementary Figures 1 to 18

1. Materials.

3,4-dimethoxybenzoic acid ($\geq 98\%$, Aldrich) and 1,2-dimethoxybenzene ($\geq 98\%$, Aldrich), N, N-dimethylformamide ($\geq 98\%$, Aldrich) Cu(OAc)₂ ($\geq 99\%$, Aldrich) and methanol ($\geq 98\%$, Aldrich) were used as received without further purification. CO₂ and N₂ with a purity of 99.99% was purchased from Shenzhen Huatepeng Special Gas Co., LTD.

2. Electrode Synthesis and Structural Characterization

Synthesis of CuDBC: The synthesis of 8OH-DBC was followed as reported in the literature.¹⁻² 8.6 mg of 8OH-DBC ligand and 6 mg of Cu(OAc)₂·H₂O were dispersed in 500 μ L degassed dimethylformamide (DMF) and 2 mL degassed deionized water by ultrasonic treatment for 30 min. This vial was placed in 85 °C oven for 72 h. The reactant was washed with water and acetone several times and dried overnight in vacuum at room temperature to obtain the black product.

Synthesis of PA-CuDBC-1 and PA-CuDBC-2: The as-prepared Cu-DBC precursor was furtherly activated using high energy plasma treatments with 100W O₂ for 20 minutes, which was denoted as PA-CuDBC-1. Cu-DBC precursor was also treated with 100W O₂ plasma for 40 minutes, which was denoted as PA-CuDBC-2.

3. Materials characterization

Linear sweep voltammograms (LSV) were chronicled with electrochemical workstation (Princeton Applied Research 263A). Potentiostatic electrolysis were performed via a CHI 660C electrochemical station (Shanghai Chenhua). Gas-phase reduction products were detected by Gas Chromatography (SHIMADZU, GC-2014).

Microstructure images and energy dispersive X-ray spectroscopy (EDX) were obtained by field emission scanning electron microscope (FE-SEM, FEI JEOL-7800F)

and high-resolution transmission electron microscope (HR-TEM, JEM-2100F). Fourier transform infrared spectroscopy (FT-IR) was carried out by Thermo Scientific iS50 with the spectral range of 50–4600 cm^{-1} . N_2 adsorption-desorption was taken using a Micromeritics ASAP 2460 instrument with outgassing samples under vacuum at 523K for 15 h. X-ray diffraction (XRD) patterns were performed with a Rigaku MiniFlex 600 powder diffractometer using $\text{Cu K}\alpha$ radiation ($\text{k} = 1.5406 \text{ \AA}$). X-ray photoelectron spectra analysis (XPS) of Cu, O and C elements were acquired with ThermoVG Scientific ESCALAB 250 X-ray photoelectron spectrometer (Thermo Electron, U.K.) using $\text{Al K}\alpha$ X-ray source. The local atomic structure was measured by electron paramagnetic resonance (EPR). It was carried out by a Bruker ECS-EMX X-band EPR spectrometer at the room temperature of 300 K.

4. Electrochemical measurements

Electrochemical tests: PA-CuDBC-1 and all the other catalysts were tested using typical powdering and binding method in a typical H-type cell. To produce a working electrode, catalyst ink that was prepared by dispersed 10 mg catalysts in the mixed solution of 5 mL isopropanol. Then, 10 μL 5% Nafon was dropped on carbon paper (Toray) to get a loading amount of 1 mg cm^{-2} . This catalyst/carbon paper would be used as the cathode for CO_2 electrolysis. Electrolysis was tested in a typical divided electrochemical cell separated by anion exchange membrane between anode and cathode chamber in N_2 or CO_2 -saturated 0.5 M KHCO_3 aqueous solution, with Pt mesh as the counter electrode and an Ag/AgCl as reference electrode.

All potentials in this paper were transformed to reversible hydrogen electrode (RHE) by the following Nernst equation:

$$E(\text{RHE}) = E(\text{Ag}/\text{AgCl}) + 0.197 + 0.059 \times \text{pH} \quad (1)$$

Calculation of faradaic efficiency: The electrolyzer outlet was directly connected to the gas-sampling loop of the gas chromatograph (SHIMADZU, GC-2014) outfitted with a thermal conductivity detector (TCD) and a flame ionization detector (FID). The faradaic efficiencies of all products were calculated from the total amount of charge (Q/C) passed through the catalysts and the total amount of product (n/mol). $Q=I \times t$, where I is the reduction current at a specific applied potential, and t is the time for the constant reduction current, F is the Faraday constant (96,500 C/mol).³ For example, the faradaic efficiency (FE) of CO can be calculated as following equation:

$$\text{Faradaic efficiency} = 2F \times n_{CO} / (I \times t) \quad (2)$$

5. DFT calculations

DFT calculations: The DFT calculations were performed with VASP package with PBE functionals.⁴⁻⁶ All the model structures were fully relaxed till all the forces were less than 0.01 eV/Å. The adsorption energy was calculated with the following equation:

$$E = E_{final} - E_{substrate} - E_{adsorbate}$$

E , E_{final} , $E_{substrate}$ and $E_{adsorbate}$ are adsorption energy of adsorbed intermediates (*COOH, *CO, *CHO) on substrate (Cu-O₄-C, Cu-O₃-C and Cu-O₂-C doped graphene nanosheet), total energy of adsorbate on the substrate, total energy of the substrate, and total energy of the adsorbate.

The free energy of the reaction was calculated via the following equation:

$$\Delta G = E + \Delta ZPE - T\Delta S$$

ΔG , ΔZPE and ΔS represent Gibbs free energy, zero point energy and entropy, respectively.

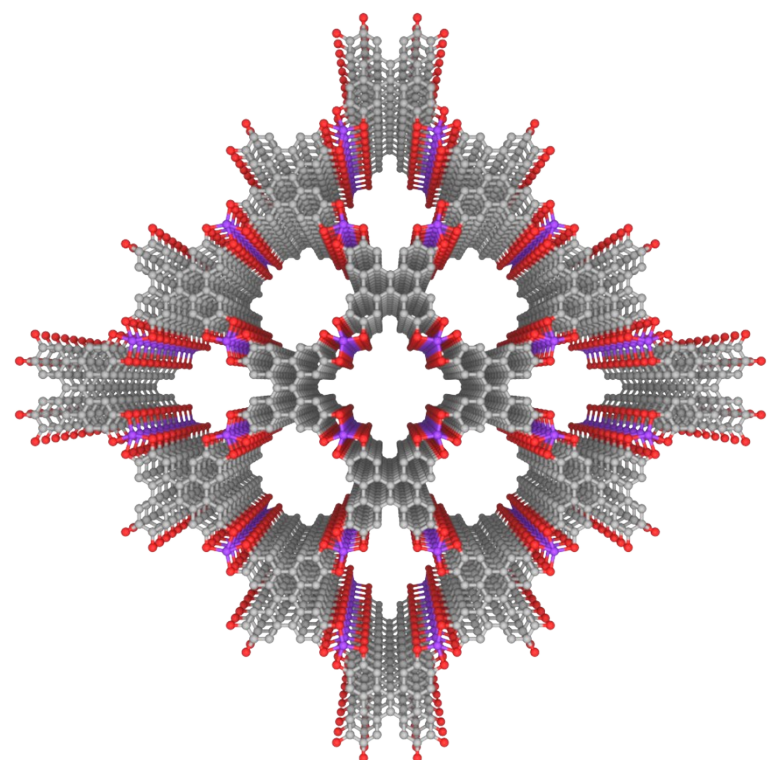


Fig. S1. The molecular structure of CuDBC.

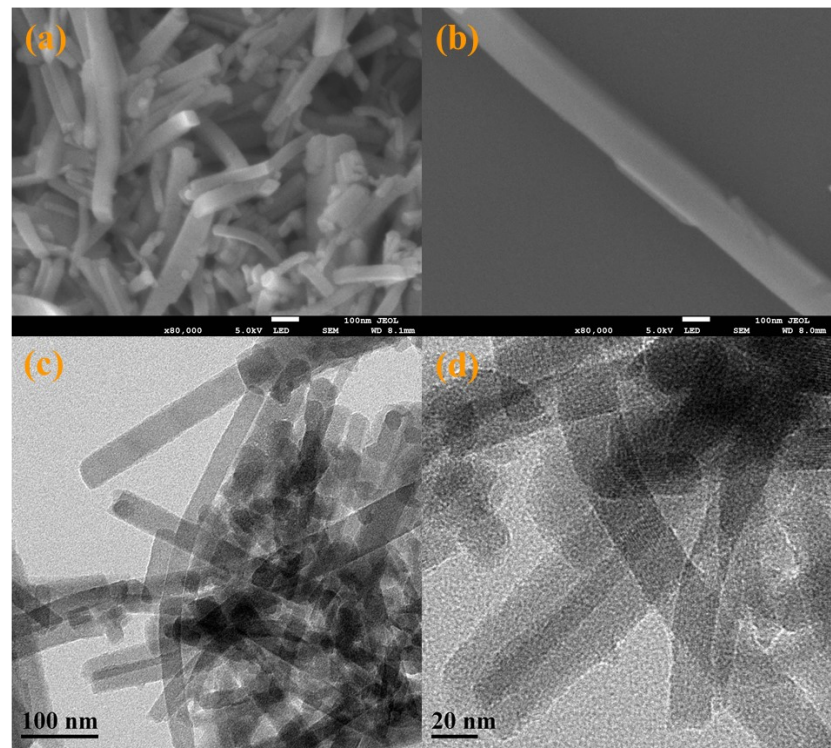


Fig. S2. SEM (a-b) and TEM (c-d) images of CuDBC.

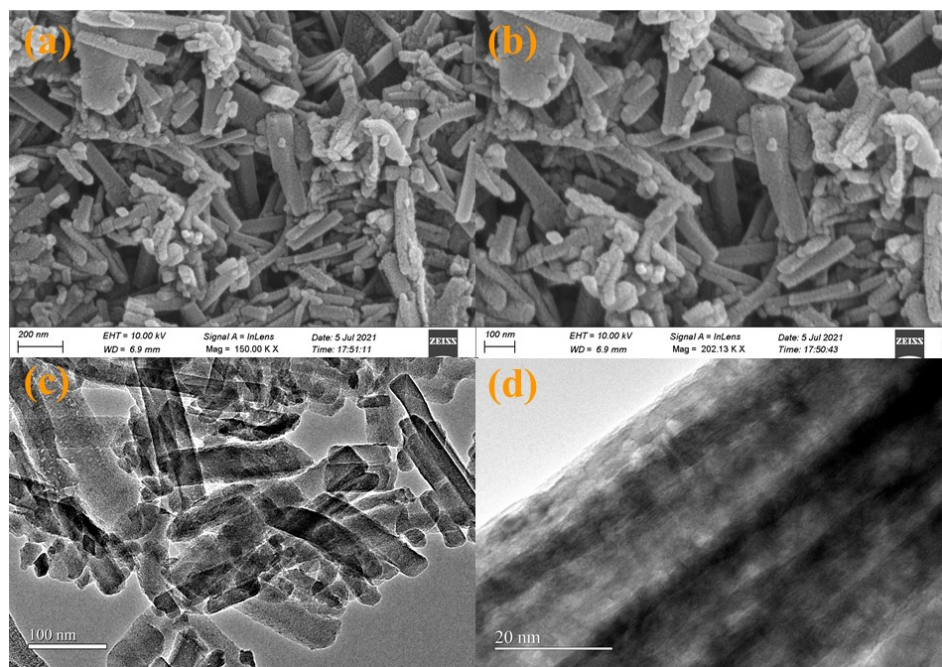


Fig. S3. SEM (a-b) and TEM (c-d) images of PA-CuDBC-1.

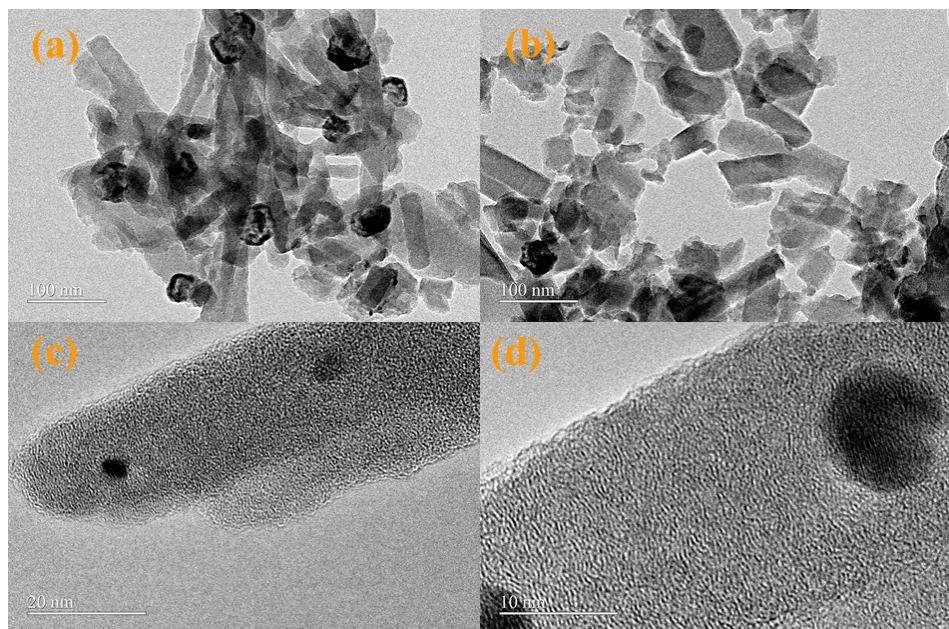


Fig. S4. TEM images of PA-CuDBC-2.

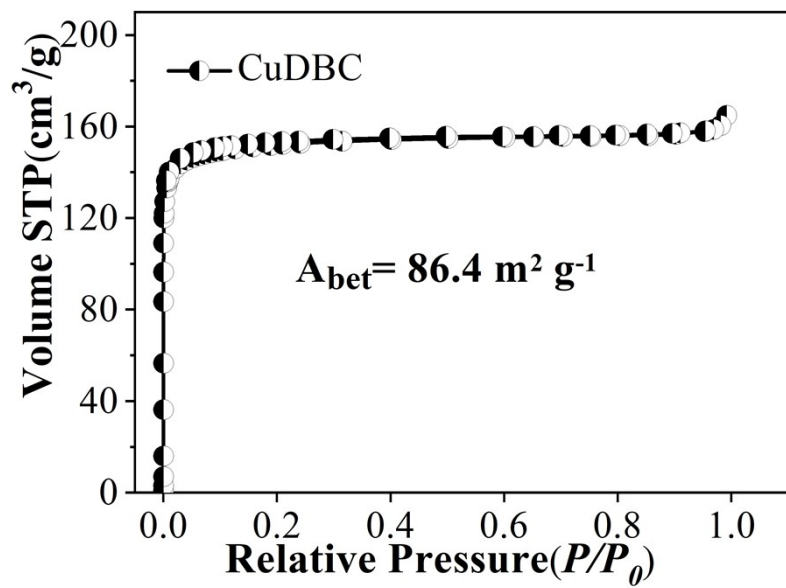


Fig. S5. N_2 adsorption–desorption isotherms of CuDBC.

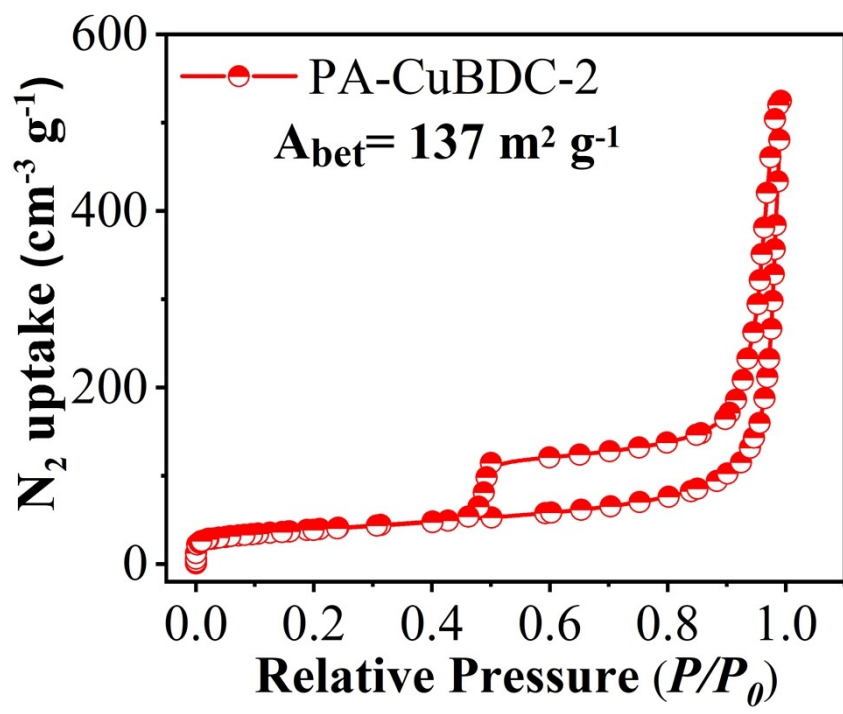


Fig. S6. N_2 adsorption–desorption isotherms of PA-CuBDC-2.

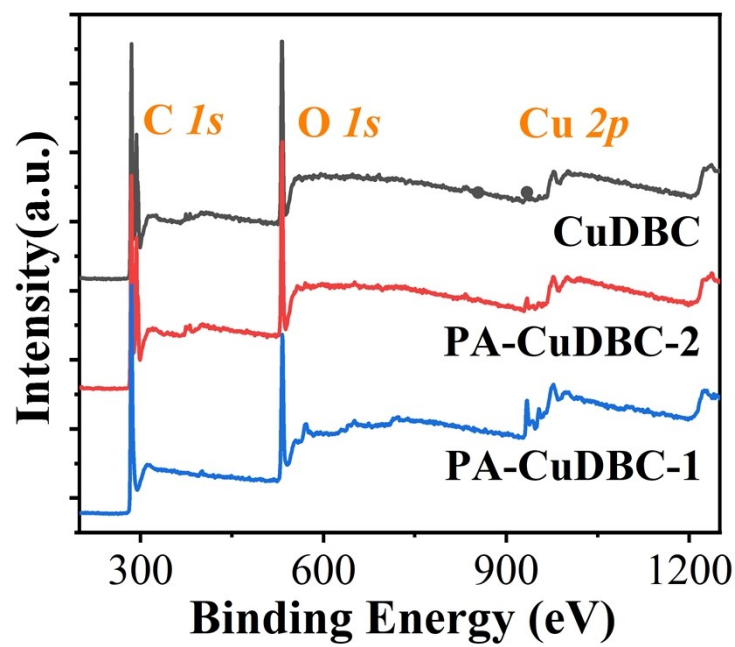


Fig. S7. XPS survey spectra of three samples.

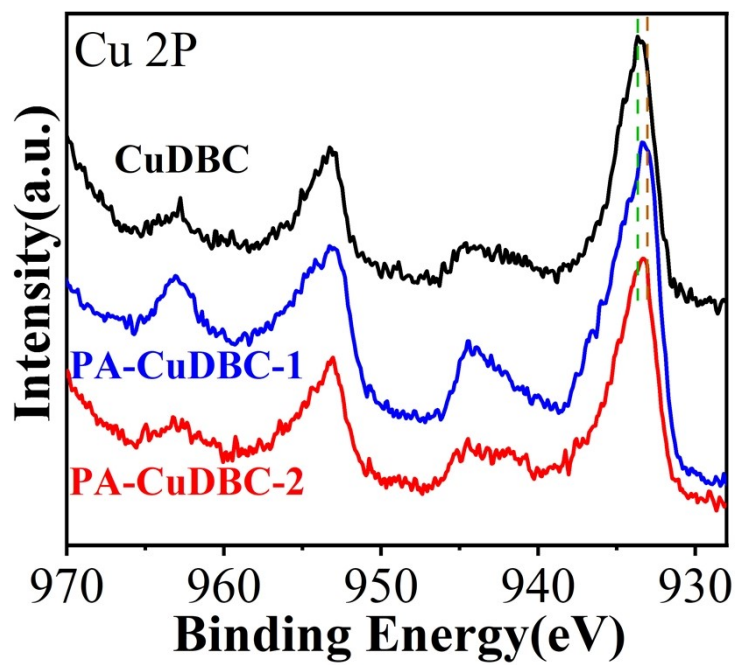


Fig. S8. Cu 2p XPS survey spectra of three samples.

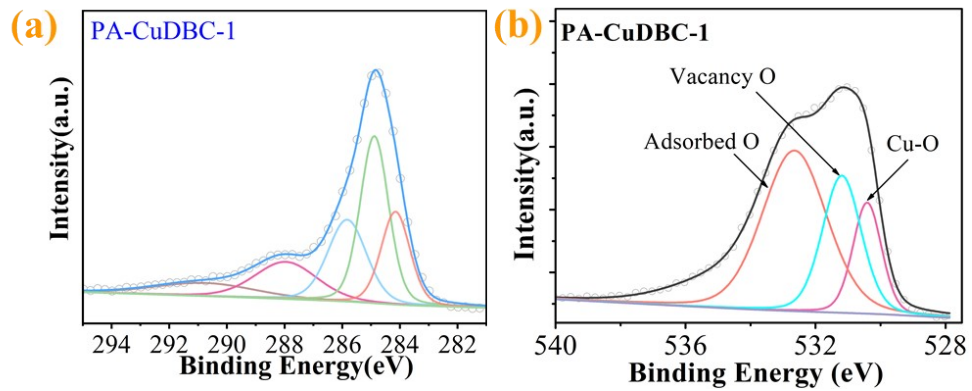


Fig. S9. (a) C 1s and (b) O 1s XPS spectra of PA-CuDBC-1.

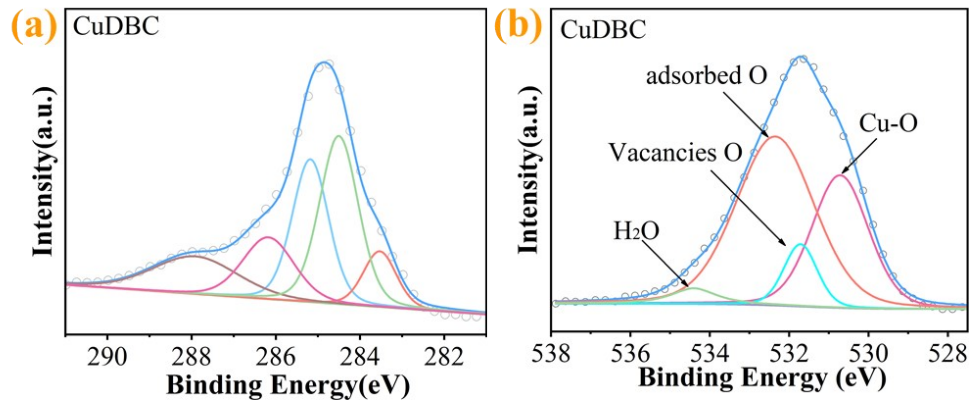


Fig. S10. (a) C 1s and (b) O 1s XPS spectra of CuDBC.

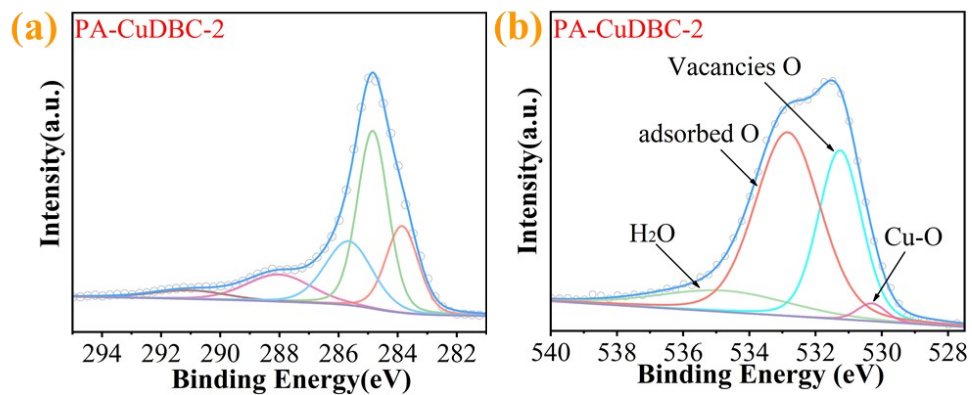


Fig. S11. (a) C 1s and (b) O 1s XPS spectra of PA-CuDBC-2.

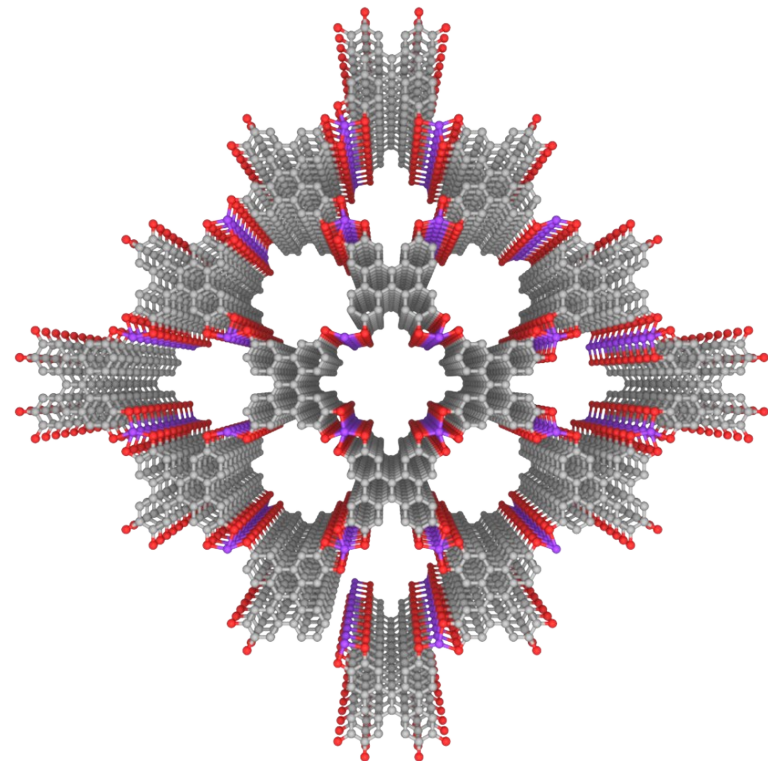


Fig. S12. The molecular structure of CuDBC after plasma activation.

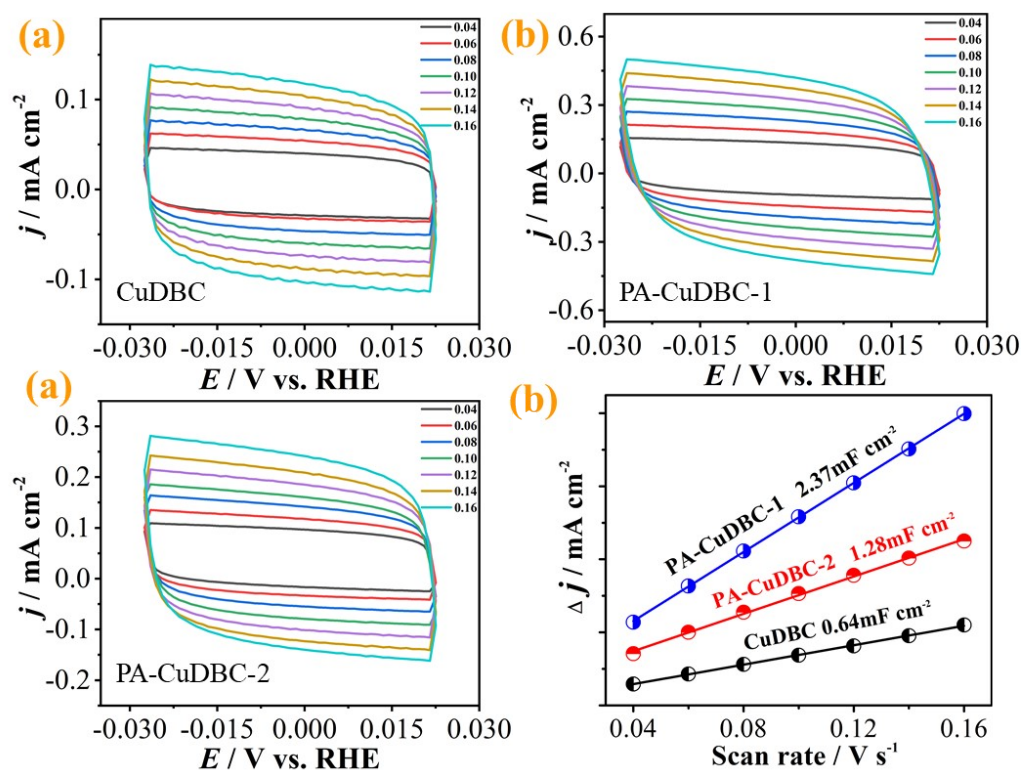


Fig. S13. CV curves of three samples in the double layer region.

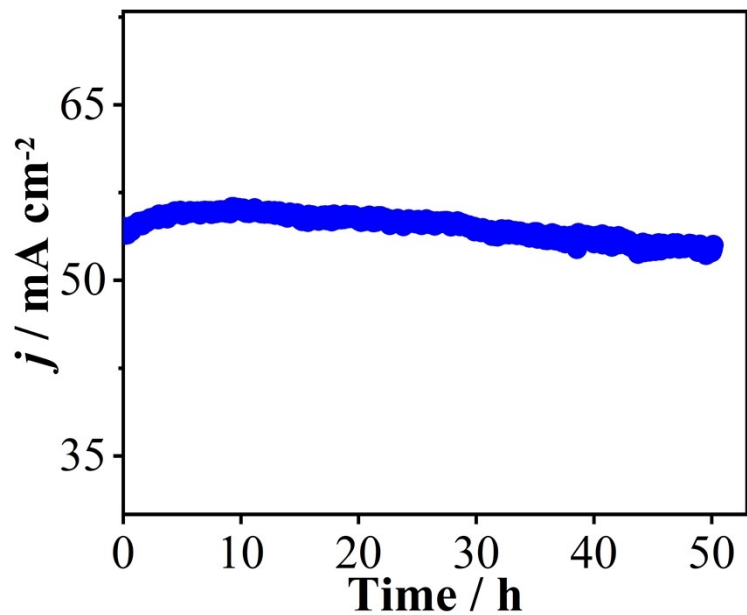


Fig. S14. Long-term tests of PA-CuDBC-1 at -1.1 V_{RHE} in CO₂-saturated 0.5 M KHCO₃ electrolyte.

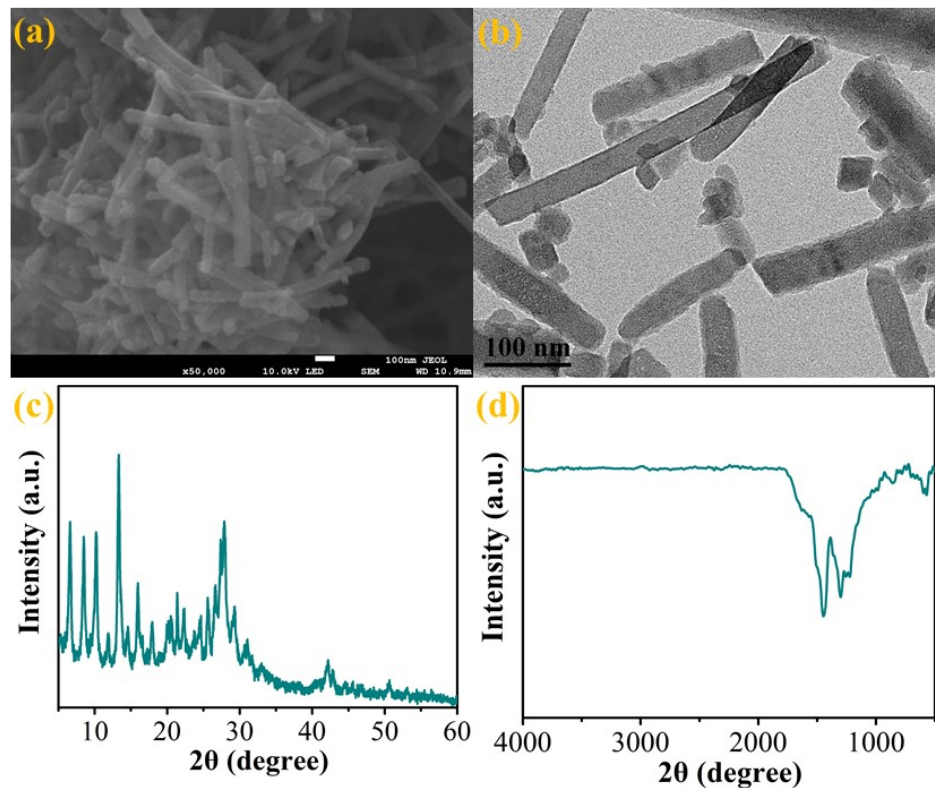


Fig. S15. SEM, TEM, XRD and FTIR analysis (a-d) of the PA-CuDBC-1 sample after all the electrolysis.

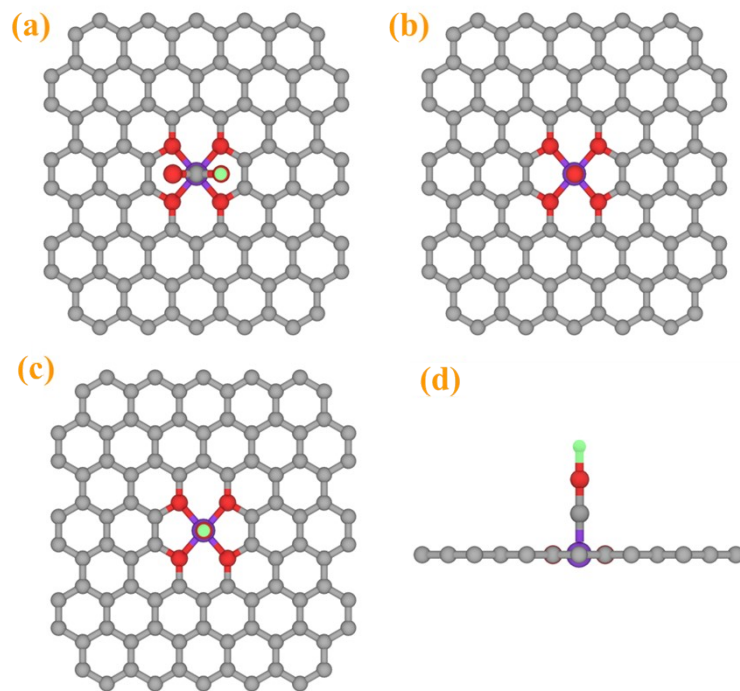


Fig. S16. Up and side view for the structure model of Cu-O₄-C graphene adsorbed with *COOH, *CO and *CHO intermediates.

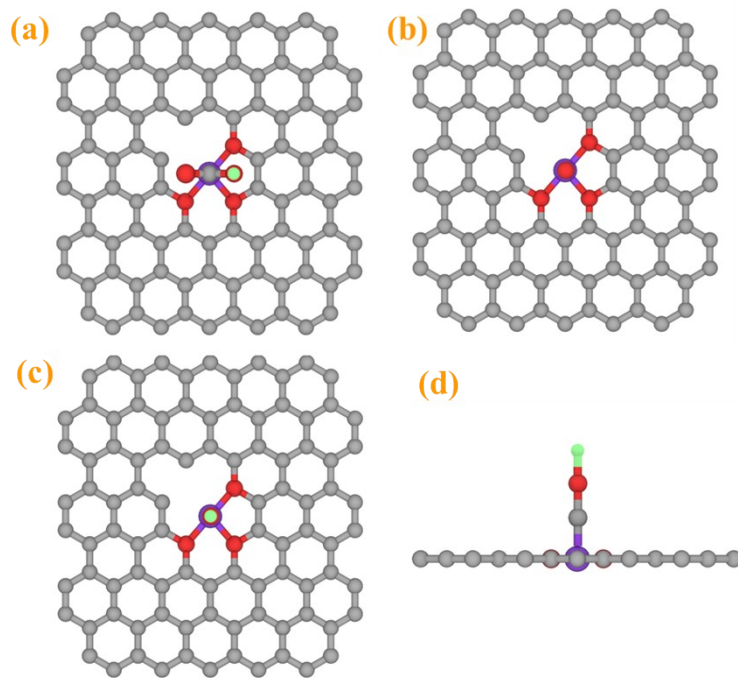


Fig. S17. Up and side view for the structure model of Cu-O₃-C graphene adsorbed with *COOH, *CO and *CHO intermediates.

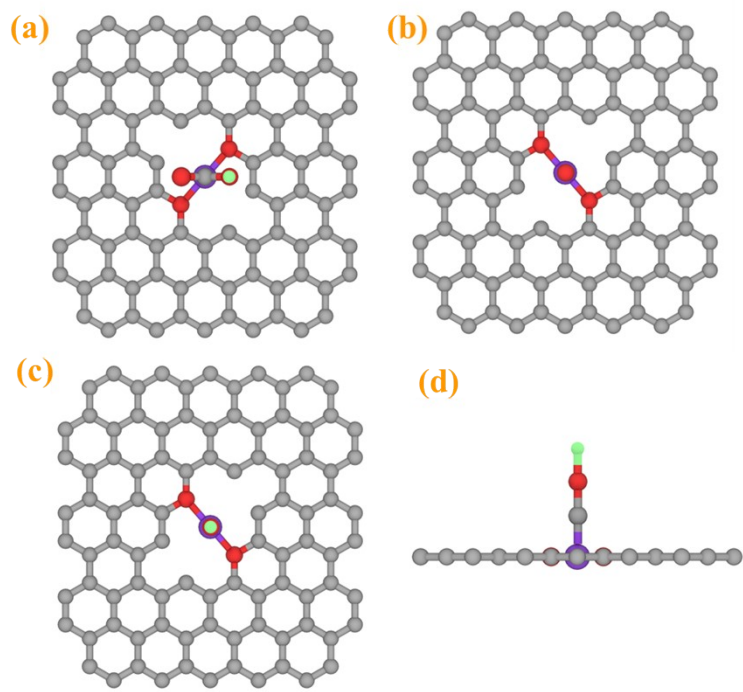


Fig. S18. Up and side view for the structure model of Cu-O₂-C graphene adsorbed with *COOH, *CO and *CHO intermediates.

Reference

- 1 S. K. Varshney, H. Nagayama, H. Takezoe, V. Prasad, *Liq. Cryst.*, **2009**, 36, 1409.
- 2 J. Liu, Y. Zhou, Z. Xie, Y. Li, Y. Liu, J. Sun, Y. Ma, O. Terasaki, L. Chen, *Angew. Chem.*, **2020**, 132, 1097–1102.
- 3 S. Gao, Y. Lin, X. Jiao, Y. Sun, Q. Luo, W. Zhang, D. Li, J. Yang, Y. Xie, *Nature*, **2016**, 529, 68–72.
- 4 G. Kresse, J. Furthmüller, *Comput. Mater. Sci.*, **1996**, 6, 15.
- 5 J. J. Mortensen, L. B. Hansen, K. W. Jacobsen, *Phys. Rev. B*, **2005**, 71, 035109.
- 6 J. P. Perdew, K. Burke, M. Ernzerhof, *Phys. Rev. Lett.*, **1996**, 77, 38651.